

A Simple Quantum Model of Ultracold Polar Molecule Collisions

Zbigniew Idziaszek

Faculty of Physics, University of Warsaw, 00-681 Warsaw, Poland

Goulven Quémener and John L. Bohn

JILA, NIST and University of Colorado, Boulder, CO, 80309-0440, USA

Paul S. Julienne

Joint Quantum Institute, NIST and the University of Maryland, Gaithersburg, MD 20899-8423, USA

(Dated: October 31, 2018)

We present a unified formalism for describing chemical reaction rates of trapped, ultracold molecules. This formalism reduces the scattering to its essential features, namely, a propagation of the reactant molecules through a gauntlet of long-range forces before they ultimately encounter one another, followed by a probability for the reaction to occur once they do. In this way, the electric-field dependence should be readily parametrized in terms of a pair of fitting parameters (along with a C_6 coefficient) for each asymptotic value of partial wave quantum numbers $|L, M\rangle$. From this, the electric field dependence of the collision rates follows automatically. We present examples for reactive species such as KRb, and non-reactive species, such as RbCs.

PACS numbers: 34.50.Cx, 34.50.Lf

Ultracold molecules present researchers with unique physical systems that are a curious mixture of small and large energies, and of tiny and enormous length scales. Thanks to recent experimental advances, certain molecules can be prepared in specific hyperfine states, even though they are separated in energy only by $\sim 10^{-9}$ eV [1–3]. Yet, upon colliding, these same molecules explore the ~ 1 eV energies afforded by their electronic potential energy surfaces. Similarly, the translational kinetic energy of these molecules, set by their temperature T , can be as small as $k_B T \sim 10^{-11}$ eV. At these energies the force the molecules exert on one another can be significant on length scales that are orders of magnitude larger than the molecules themselves. Because long-range dipolar forces are experimentally controllable, there has been much discussion about the prospect of either limiting or enhancing chemical reaction rates by the simple artifice of changing an electric field [4]. Indeed, an effect of this kind has been dramatically demonstrated and explained recently [5]. Collisions of ultracold molecules are thus, in principle, remarkably complicated systems to understand in detail. On the one hand, every degree of freedom is involved, from the hyperfine states in which the molecules are prepared to the complete re-arrangement of molecules in a chemical reaction. On the other hand, the actual number of observables may be rather small, consisting perhaps of a handful of loss rate coefficients. The long path connecting complex molecular Hamiltonians to what is actually seen in the lab may indeed prove intractable from *ab initio* theory.

For this reason, it is worthwhile to find simple formulations of collision theory at ultralow temperatures, especially formulations that naturally take advantage of the vast differences in energy and length scales present [6, 7]. Recently, two complementary approaches have accounted fairly well for experiments that have observed ultracold

chemical reactions of fermionic KRb molecules. In the first, a multichannel quantum defect theory (MQDT) approach has successfully replaced the short-range physics by suitably parametrized boundary conditions that acknowledge both a scattering phase shift and the probability of chemical reaction [8]. The boundary conditions were matched to highly accurate solutions of the long-range scattering, which in fact were carefully characterized analytically, allowing for simple analytic formulas for scattering observables [6]. The second, “quantum threshold” (QT) approach focused on the fact that the molecules had to tunnel through a centrifugal barrier with a given probability, which varied with energy in accord with the Wigner threshold laws [9]. By floating the value of the tunneling probability at the barrier’s peak, this method was able to describe in an analytic way the chemical reaction probability even in the presence of an electric field that polarized the molecules [5].

In this Rapid Communication we merge the ideas behind these approaches to arrive at a consistent theory of ultracold polar molecule collisions. We will exploit the short-range parametrization already afforded by the zero-field MQDT approach, complemented by a numerical treatment of long-range wave function propagation. One main result is the classification of molecules according to whether their scattering is universal, with loss rates that depend only on purely long-range features of the potential energy surfaces; or else non-universal, containing resonances that carry more detailed information about specifics of the interactions. These kinds of field-dependent resonances were reported previously [10–16]. We find that the locations and contrast of these features are specified once the MQDT parameters of the short-range physics are given. Therefore, a whole swath of the electric-field-dependent collisional spectrum may be simply characterized.

We begin with the Hamiltonian for interaction of two dipolar molecules in well-defined single internal states, with reduced mass μ and intermolecular separation R :

$$H = T_r + V_{\text{sr}} + V_{\text{cent}} + V_{\text{vdW}} + V_{\text{dd}}. \quad (1)$$

Here, T_r is the radial kinetic energy; $V_{\text{cent}} = \hbar^2 L(L+1)/2\mu R^2$ is the centrifugal energy corresponding to partial wave L ; $V_{\text{vdW}} = -C_6/R^6$ is the van der Waals interaction between two molecules, here assumed isotropic; and $V_{\text{dd}} = C_3(L, L'; M_L)/R^3$ is the dipole-dipole interaction between the molecules, which couples different partial waves, but which preserves the projection M_L of this angular momentum onto the field axis [9]. These three terms identify the long-range physics, denoted collectively as V_{lr} . In addition, V_{sr} incorporates all short-range physics, such as elastic and inelastic scattering, possible resonances to ro-vibrationally excited molecular states, or even chemical reaction. We will not deal explicitly with V_{sr} in what follows.

For the present, we are interested in collisions that may result in chemical reactions, rather than hyperfine-changing collisions. We therefore ignore all other hyperfine states besides the incident ones. (The theory can be adapted to include these later, however.) In our model, scattering via the Hamiltonian (1) is then a multi-channel problem, where the channels are defined by the partial wave quantum numbers L . Higher values of L generate higher centrifugal barriers, and thus inhibit the passage of the molecules to short range where they can react. Therefore, only a handful of L 's are necessary to describe chemical quenching phenomena at ultralow temperatures. In fact, we consider a *single* potential that is constructed by diagonalizing V_{lr} in the partial wave basis at each value of R , in the spirit of the Born-Oppenheimer approximation, as in Ref. [16].

We therefore reduce the problem to scattering in a single potential, albeit one from which wave function flux can leak at small values of R . Within this model, the scattering consists of three parts: 1) molecules approach one another and transmit some fraction of their incident flux through the long-range potential V_{lr} , to arrive at an intermediate separation R_0 ; 2) the molecules enter into the near zone, where they may either react (in which case flux is lost) or else scatter back into the channel from which they came, generating a phase shift; 3) what's left of the molecular flux proceeds to infinite R and counts toward elastic scattering. In either event, scattering is defined via the diagonal scattering matrix element in our potential, S , whose magnitude may be less than unity if a reaction has occurred. Quite generally, elastic and quenching scattering rate constants are given, respectively, by

$$\begin{aligned} K^{\text{el}}(E) &= g \frac{\pi \hbar}{\mu k} |1 - S(E)|^2 \\ K^{\text{qu}}(E) &= g \frac{\pi \hbar}{\mu k} (1 - |S(E)|^2), \end{aligned} \quad (2)$$

where k is the incident wave number, and $g = 1, 2$ according as the particles are indistinguishable or distinguishable in their initial channel.

The S-matrix is characterized by a complex phase shift via $S = e^{2i\eta}$, which defines the complex, energy-dependent scattering length

$$\tilde{a}(k) = \tilde{\alpha}(k) - i\tilde{\beta}(k) = -\frac{\tan \eta(k)}{k}. \quad (3)$$

The real power of the quantum defect approach is that it provides *analytic* expressions for the complex scattering length for zero-electric-field collisions [17]. This follows from a careful parametrization of standard wave functions in the long-range potential, which is assumed to consist solely of van der Waals plus centrifugal potentials. As was shown in Ref. [8], the scattering lengths for the lowest partial waves simplify, in the limit $k\tilde{a} \ll 1$, to

$$\begin{aligned} \tilde{a}_{L=0} &= a + \bar{a}y \frac{1 + (1-s)^2}{i + y(1-s)} \\ \tilde{a}_{L=1} &= -2\bar{a}_1(k\bar{a})^2 \frac{y + i(s-1)}{ys + i(s-2)}. \end{aligned} \quad (4)$$

Here several scale parameters are used, such as the Gribakin-Flambaum mean scattering length $\bar{a} = 2\pi(2\mu C_6/\hbar^2)^{1/4}/\Gamma(1/4)^2$, and its p -wave analogue $\bar{a}_1 = \bar{a}\Gamma(1/4)^6/(144\pi^2\Gamma(3/4)^2) = 1.064\bar{a}$. The parameters that are specific to each particular scattering problem are instead the real part of the zero-energy scattering length, a , also given in its reduced form $s = a/\bar{a}$; and the effective short-range channel coupling strength y . In the quantum-defect point of view, y stands for the probability of chemical reaction once the molecules get close together: when $y = 0$, chemical reactions are forbidden, and the scattering is purely elastic; whereas when $y = 1$, reactions occur with maximum probability [8].

Thus the parametrization of scattering observables follows as given above, whereas the actual values of the parameters s and y will vary from one molecule to the next, and may be determined by fitting experimental data. Within the theory, their values follow ultimately from the value and derivative of the total wave function $\psi(R_m)$ at a matching radius R_m . In MQDT, R_m represents the boundary between long and short-range, or equivalently small and large energy scales in the relative motion of the molecules. Its value is conveniently chosen to be smaller than the characteristic length \bar{a} , yet larger than the scale of any significant short-range physics or chemistry.

We come now to the main point of this article. At the matching point R_m , the interaction potential is sufficiently deep that the potential, and more importantly the wave function $\psi(R_m)$, are unaffected by turning the electric field on. This reflects the physical fact that laboratory strength fields, inducing energies on the order of 10^{-5} eV by polarizing the molecules, has no effect whatsoever on the eV-scale chemical reaction processes, or the perhaps 0.1 eV depth of the interaction potential at R_m . Therefore the parameters s and y can be defined once, at

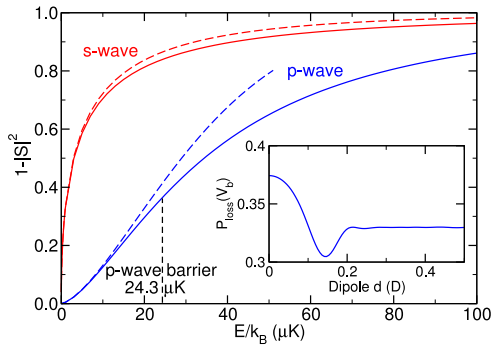


FIG. 1: (Color online) Probability to tunnel to short range, versus collision energy, for s - and p -wave collisions of KRb molecules, assuming zero electric field and $C_6 = 16130$ a.u. [15]. The dashed lines are the analytic, low-energy approximations $1 - \exp(-4k\beta)$. Inset: Dependence of the transmission probability, evaluated at the height of the centrifugal barrier, as a function of induced dipole moment d .

zero electric field, and then used at all subsequent, higher fields. It only remains to propagate the wave function ψ from R_m out to infinity. This part of the process is necessarily numerical, since the MQDT parameters for a mixed van der Waals-plus-dipole interaction are not yet characterized, and in any event are likely to be available only numerically.

In this way the entire field-dependent scattering behavior in contemporary experiments can be succinctly summarized. To set this discussion in context, we first consider the transfer function, i.e., the probability that the incident flux reaches R_m at all, in zero electric field. This function is given by the loss probability $P_{\text{loss}} = 1 - |S|^2$, evaluated for unit short-range absorption probability $y = 1$. It is shown in Fig. 1 for cold collisions of KRb molecules in zero field, for both s - and p -wave collisions. In both cases, the low-energy behavior of P_{loss} must follow the Wigner threshold laws. In the higher-energy limit, P_{loss} asymptotes to unity, since the molecules can then barrel past the comparatively weak long-range forces. The dashed lines show approximate transfer functions that incorporate the lowest-order complex scattering length from (4), namely, $\beta_0 = \bar{a}$ for s -waves and $\beta_1 = \bar{a}_1(k\bar{a})^2$ for p -waves. These approximations are adequate up to the characteristic energies $E_0 = \hbar^2/2\mu\bar{a}^2$ for s -waves, and $E_1 = (4\hbar^6/(27\mu^3C_6))^{1/2}$ for p -waves (corresponding to the height of the p -wave centrifugal barrier). For example, for the KRb molecules considered in Fig. 1, $E_0 = 98\mu\text{K}$ and $E_1 = 24.3\mu\text{K}$.

In the very low energy limit for p -waves, the quantum threshold model in Ref. [9] also yields the correct low-energy behavior of P_{loss} , and indeed is based on the Wigner laws. The only remaining ingredient within this model is to normalize P_{loss} to its correct value at the height of the p -wave centrifugal barrier. This

value, $P_{\text{loss}}(V_b) = 0.37$, is also indicated in the figure, and it is a universal value that is independent of the specific C_6 or reduced mass of the collision partners. In the QT model the transmission function is given as $P_{\text{loss}} = P_{\text{loss}}(V_b)(E/V_1)^{3/2}$. Based on this single fit parameter $P_{\text{loss}}(V_b)$, the QT model is therefore a reasonable approximation to collisions with unit absorption (or finite absorption, by multiplying by an additional absorption probability). Moreover, it is easy to evaluate at nonzero fields, by simply evaluating V_b for the correct adiabatic curve. To a good approximation, the factor $P_{\text{loss}}(V_b)$ is only weakly-dependent on the electric field strength, as shown in the inset to Fig. 1.

This weak dependence can be seen, at least qualitatively, by replacing the actual barrier by an artificial inverse Morse potential, constructed so as to have the same curvature at its barrier maximum as the actual potential $\hbar^2 L(L+1)/(2\mu R^2) - C_n/R^n$. The inverse Morse potential model can then be solved analytically as a transmission problem [18], to yield $P_{\text{loss}}(V_b) = (1 - e^{-4\pi f})/2$, where $f = \sqrt{L(L+1)2(n-2)}/n$. This approximation correctly shows that the result is independent of the long-range coefficient C_n , as well as the reduced mass, but that it does depend on the partial wave l as well as the character n of the long-range potential. It also shows that, coincidentally, the transfer function at the barrier height is the same for a van der Waals potential $n = 6$ and for a dipole potential $n = 3$, for p -wave collisions. Thus a weak dependence of $P_{\text{loss}}(V_b)$ on electric field is perhaps not unexpected. For s -wave collisions, in which the long-range dipole potential scales as C_4/R^4 [19], we would expect a stronger variation of $P_{\text{loss}}(V_b)$ with electric field.

Based on these remarks, we turn now to the electric field dependence of reactive collisions, making the assumption that s and y are independent of field. Doing so, a numerical calculation readily produces the reaction rate constant versus the dipole moment of the colliding species. Examples are shown in Fig. 2 for identical fermions (odd partial waves, Fig. 2a) and identical bosons (even partial waves, Fig. 2b). In both cases, the overall tendency is for the rates to rise as the field is turned on. This rise is, however, more dramatic for identical fermions, which are suppressed in zero-field by the van der Waals centrifugal barrier.

The most striking feature in these figures is the presence or absence of resonance-like features as the dipole is increased. For weak short-range absorption (e.g., $y = 0.1$), these features are pronounced, and fall into regular patterns according to the angular momentum L , M of the dominant partial wave. For $L > 0$ these are shape resonances behind field-dependent centrifugal barriers, while for $L = 0$ these resonances appear as the effective long-range potential is systematically deepened to include additional bound states [11, 16]. Vice versa, in the limit of strong short-range absorption (e.g., $y = 1$), these features are completely washed out. This occurs because, at complete unit absorption, the resonant state

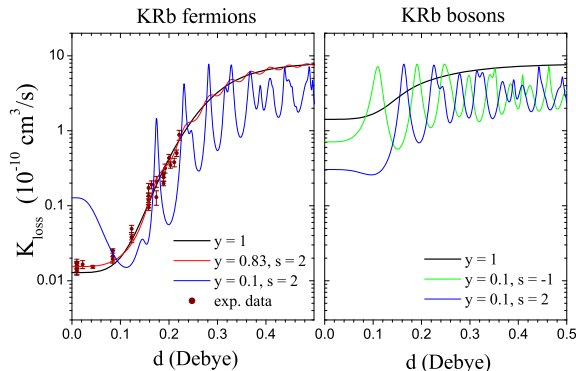


FIG. 2: (Color online) Dependence of chemical reaction rates K_{loss} on dipole moment d for identical fermionic (a) or bosonic (b) KRb molecules. In the case of unit reaction probability, $y = 1$, this variation takes a universal form independent of details of the short-range physics. For $y < 1$, non-universal resonances appear that reveal more details of the short-range interaction. The data from [5] (points) are well-fit by near-universal scattering, $y = 0.83$

decays immediately; it does not survive for even a single period of the resonance.

The presence or absence of these resonances thus contains information on the scattering, and in particular on the value of y . Consider, for example, KRb molecules, which are chemically reactive at zero temperature [20, 21], and should thus possess large absorption probabilities y . The points in Fig. 2a show the data from the KRb experiment [5]. The best fit value to these data yields $y = 0.83$, consistent with large, if not perfect, absorption (red line). Interestingly, a fit to the zero-field data alone instead yields a value $y = 0.4$ [8]. Thus the electric-field dependence of reaction rates (“electric-

field spectroscopy,” [12]) is a valuable component in accurately determining the parameters that govern scattering. On the other hand, another class of molecules, typified by RbCs, are not chemically reactive at low temperature [20], and will yield $y = 0$, or very nearly so. Here the resonances should show up clearly, in either elastic scattering, hyperfine-changing collisions, or perhaps in three-body losses. Note that the resonances are likely to be quite narrow in this case [14].

When the resonances do appear, their positions result from phase shifts at short range. We illustrate this in Fig. 2b, where resonances are shown for two alternative values of s . In this figure the same value of s is used for all angular momentum channels (L, M), but in fitting real-life data this is probably not the case, and each family of resonances specified by (L, M) will likely contribute its own complex phase shift. Although the overall positions of the resonances are not specified, nevertheless their relative spacings follow a specific pattern. For example, for s -wave resonances the location in field $\mathcal{E}(n)$ of the n -th resonance takes the form [12]

$$\mathcal{E}(n) = \mathcal{E}' \sqrt{\frac{n_0 + n}{n_\infty - n}}, \quad (5)$$

where \mathcal{E}' is an overall scaling, n_∞ is related to the scattering phase shift at threshold, and n_0 is akin to a short-range quantum defect parameter. This approximation was derived using semiclassical arguments, which are also applicable to the higher-partial wave case [14]. The fully quantum treatment described here should afford an accurate, complete parametrization of these features.

We gratefully acknowledge support from an AFOSR MURI on Ultracold Molecules, and a Polish Government Research Grant

-
- [1] K.-K. Ni, S. Ospelkaus, M. Miranda, A. Peer, B. Neyenhuis, J. Zirbel, S. Kotochigova, P. Julienne, D. Jin, and J. Ye, *Science* **322**, 231 (2008).
 - [2] S. Ospelkaus, K.-K. Ni, G. Quémener, B. Neyenhuis, D. Wan, M. H. G. de Miranda, J. L. Bohn, J. Ye, and D. S. Jin, *Phys. Rev. Lett.* **104**, 030402 (2010).
 - [3] J. G. Danzl, M. J. Mark, E. Haller, M. Gustavsson, R. Hart, J. Aldegunde, J. M. Hutson, and H.-C. Nägerl, *Nat. Phys.* **6**, 265 (2010).
 - [4] T. V. Tscherbul and R. V. Krems, in *Cold Molecules: theory, Experiment, Applications*, edited by R. V. Krems, W. C. Stwalley, and B. Friedrich (CRC Press, 2009), chap. 4, pp. 125–168.
 - [5] K.-K. Ni, S. Ospelkaus, D. Wang, G. Quémener, B. Neyenhuis, M. H. G. de Miranda, J. L. Bohn, J. Ye, and D. S. Jin, *Nature* **464**, 1324 (2010).
 - [6] B. Gao, E. Tiesinga, C. J. Williams, and P. S. Julienne, *Phys. Rev. A* **72**, 042719 (2005).
 - [7] J. P. Burke, J. L. Bohn, and C. H. Greene, *Phys. Rev. Lett.* **81**, 3355 (1998).
 - [8] Z. Idziaszek and P. S. Julienne, *Phys. Rev. Lett.* **104**, 113202 (2010).
 - [9] G. Quémener and J. L. Bohn, *Phys. Rev. A* **81**, 022702 (2010).
 - [10] B. Deb and L. You, *Phys. Rev. A* **64**, 022717 (2001).
 - [11] C. Ticknor and J. L. Bohn, *Phys. Rev. A* **72**, 032717 (2005).
 - [12] J. L. Bohn and C. Ticknor, in *Proceedings of the XVII International Conference on Laser Physics*, edited by E. A. Hinds, A. Ferguson, and E. Riis (World Scientific, 2005), p. 207.
 - [13] C. Ticknor, *Phys. Rev. A* **76**, 052703 (2007).
 - [14] V. Roudnev and M. Cavagnero, *J. Phys. B* **42**, 044017 (2009).
 - [15] S. Kotochigova, arXiv:1003.2672 (2010).
 - [16] V. Roudnev and M. Cavagnero, *Phys. Rev. A* **79**, 014701 (2009).
 - [17] P. S. Julienne, *Faraday Disc.* **142**, 361 (2009).
 - [18] Z. Ahmed, *Phys. Rev. A* **47**, 4761 (1993).
 - [19] A. V. Avdeenkov and J. L. Bohn, *Phys. Rev. A* **66**, 052718 (2002).

- (2002).
- [20] P. S. Żuchowski and J. M. Hutson, Phys. Rev. A **81**, 060703 (2010).
- [21] E. R. Meyer and J. L. Bohn, arXiv:1004.3317 (2010).